A lipophilic ionic liquid based on formamidinium cations and TFSI: the electric response and the effect of CO2 on conductivity mechanism

Bertasi, Federico; Giffin, Guinevere; Vezzù, Keti; Pace, Guiseppe; Abu-Lebdeh, Yaser; Armand, Michel; Di Noto, Vito

Publisher's version / Version de l'éditeur:
https://doi.org/10.1039/C7CP02304A
Physical Chemistry Chemical Physics, 2017-09-05

PCCP

Accepted Manuscript

This article can be cited before page numbers have been issued, to do this please use: F. Bertasi, G. Giffin, K. Vezzù, G. Pace, Y. Abu-Lebdeh, M. Armand and V. DI NOTO, *Phys. Chem. Chem. Phys.*, 2017, DOI: 10.1039/C7CP02304A.

ROYAL SOCIETY OF CHEMISTRY

rsc.li/pccp

View Article Online
DOI: 10.1039/C7CP02304A

Journal Name

ARTICLE

A lipophilic ionic liquid based on formamidinium cations and TFSI: The electric response and the effect of CO_2 on conductivity mechanism

Received 00th January 20xx,
Accepted 00th January 20xx

DOI: 10.1039/x0xx00000x

www.rsc.org/

Federico Bertasi[a], Guinevere A. Giffin[b], Keti Vezzù[a], Pace Giuseppe[c,d], Yaser Abu-Lebdeh[e], Michel Armand[f], Vito Di Noto*[,a,c]

The work describes the preparation of the new lipophilic ionic liquid tetraoctyl-formamidinium bis(trifluoromethanesulfonyl) imide (TOFATFSI), which is miscible with lower alkanes. In particular, this manuscript focuses on the electric behaviour of TOFATFSI in the particularly challenging highly apolar environment of supercritical CO_2. The conductivity and relaxation phenomena are revealed through the analysis of the broadband electric spectra with particular emphasis on the effect of temperature and CO_2 uptake on the IL conductivity. It is found that temperature boosts the conductivity via an increase in the charge carrier mobility. Also, CO_2 absorption affects both the conductivity and the permittivity of the material due to the presence of CO_2-IL interactions that modulate the nanostructure and the size of the TOFATFSI aggregates, which increases both the mobility and the density of the charge carriers.

Introduction

Ionic liquids (ILs) have drawn sustained attention in the last twenty years due to their unique combination of intrinsic conductivity, very low vapour pressure and their ability to be tailored to the application via facile chemical modification.[1] ILs have been extensively studied as the supporting electrolytes for lithium or sodium salts in electrochemical applications.[1-3] Most ILs are soluble/miscible in polar organic solvents, especially those ILs containing the most studied bis(trifluoromethanesulfonyl) imide (TFSI, $(CF_3SO_2)_2N^-$) anion. However, these ILs have poor solubility/miscibility in strictly apolar media like alkanes. Even the highly hydrophobic phosphonium cation $(C_6H_{13})_3P^+C_{14}H_{29}$ has no marked miscibility in hexane, neither with Cl^- nor $TFSI^-$ as counter anion. It is possible that higher solubility could be obtained when the charge delocalization is extended to more than one cationic centre (e.g. 2,3…) provided that a sufficient number (> three) of long alkyl chains are appended to the cation.

Imidazolium-based ILs can be made with two long alkyl chains attached to the nitrogen atoms, but the synthetic chemistry beyond two alkyl chains is very complex and still unexplored. Multi-arm guanidinium cations have been proposed for ILs,[4, 5] but even with four long octyl chains, only the Cl^- derivative was hexane-miscible.[6] Per-alkyl guanidinium salts are not planar due to steric hindrance within the cation and a loss of delocalization. In addition, Cl^- is far from optimal in terms of conductivity and is prone to promote corrosion. Thus our attention was focused on tetraalkyl formamidinium $[(R_2N)_2CH]^+$ as a cation, where the hydrogen atom prevents steric hindrance and the charge remains delocalized, and $TFSI^-$ as anion. Tetraoctyl-formamidinium (TOFA) TFSI proved to be a water-insoluble IL that is completely miscible with the lower alkanes and the solutions are ionic conductors. Therefore, we were intrigued if conductivity could be induced in an even more demanding medium, i.e. supercritical carbon dioxide ($scCO_2$). This paper reports the results of this investigation, where clear miscibility was observed with CO_2.

The aim of this paper is: a) to prepare a new lipophilic ionic liquid which is miscible with hydrocarbons, completely immiscible with water and other polar solvents, and which exhibits an acceptable ionic conductivity for practical application in various electrochemical devices; and b) to investigate the behaviour of the IL in this new and challenging environment, and specifically the interplay that exists between the electric response and the nanoscale interactions that influence the structure of the system. The second goal of the study is addressed by modulating the electric response of the IL, measured with broadband electrical spectroscopy (BES), through the partial pressure of CO_2 (P_{CO2}). CO_2, with a permittivity of ε_r = 1.08,[7] acts as a seed of aggregation that

[a] Section of "Chemistry for Technology" (ChemTech), Department of Industrial Engineering, University of Padova, Via Marzolo 1 in the Department of Chemical Sci-ences, 35131 Padova (Italy)
[b] Fraunhofer Institute for Silicate Research (ISC), Neu-nerplatz 2, 97082 Wuerzburg, Germany
[c] CNR-ICMATE, Via Marzolo 1, 35131, Padua, Italy
[d] Department of Chemical Sciences, University of Padova, Via Marzolo 1,35131 Padova (Italy)
[e] National Research Council Of Canada, 1200 Montreal Road Ottawa, ON K1A 0R6, Canada
[f] CIC Energigune, Parque Tecnológico de Álava, Albert Einstein, 48. 01510 Miñano, Álava, Spain
[g] * E-mail: vito.dinoto@unipd.it
See DOI: 10.1039/x0xx00000x

View Article Online
DOI: 10.1039/C7CP02304A

enhances the lipophilic behaviour of alkyl chains in the cationic aggregates and easily modulate the nano-morphology of the IL and therefore its electric response and conductivity mechanism.

Experimental

Reagents

Dioctylamine and formamidine hydrochloride were obtained from Aldrich and Alfa-Aesar, respectively. LiTFSI was a generous gift of Rhodia (now Solvay).

Synthesis of TOFATFSI

The synthesis reaction was based on a simp trans-amination reaction:

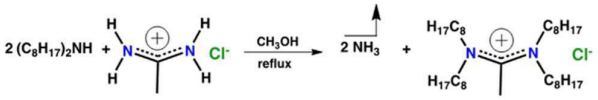

A 2:1 ratio of dioctyl amine and formamidine chloride was refluxed for eight days in methanol until no further evolution of ammonia was observable (pH paper). The methanol was removed from the solution via evaporation. TOFACl was then suspended in water and a 1.2:1 excess of LiTFSI was added (Scheme 1). The resulting dense liquid was decanted, extracted with dichloromethane (CH_2Cl_2), washed three times with water, and the excess CH_2Cl_2 was removed to yield an oily liquid.

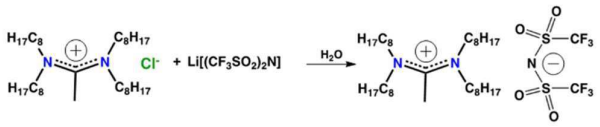

Scheme 1. Structure of tetraoctyl-formamidinium TFSI (TOFATFSI)

Instruments and Methods

Thermogravimetric (TG) analyses were performed with a high resolution TGA 2950 (TA Instruments) thermobalance using a working N_2 flux of 100 mL·min^{-1}. The TG profiles were collected in the temperature range between 25 and 800 °C. Approximately 7 mg of material were analysed in an open platinum pan. Differential scanning calorimetry (DSC) measurements were carried out in cyclic mode (two cycles) with a MDSC 2920 differential scanning calorimeter (TA Instruments) equipped with a LNCA low-temperature attachment operating under a nitrogen flux of 30 cm^3·min^{-1}. The measurements were performed with a heating rate of 3°C·min^{-1} between -150 and 70°C on about 4 mg of sample sealed in an aluminium pan. The Fourier transform infrared (FT-IR) spectrum was collected with a Nicolet FT-IR Nexus spectrometer equipped with a dry air purge at a resolution of 4 cm^{-1}.

Broadband electric spectra were collected in the frequency range from 0.01 to 10^7 Hz and the temperature range from -150 to 80°C using a Novocontrol Alpha-A analyser. The temperature was increased in 10°C increments using a home-made cryostat operating with a N_2 gas jet heating and cooling system. The temperature was measured with accuracy higher than ±0.5°C. Electrode separation was maintained by inserting two pieces of 200 µm diameter optical fibre. The geometrical cell constant was determined by measuring the electrode–electrolyte contact surface and the distance between the electrodes. No corrections for the thermal expansion of the cell were used. The complex impedance ($Z^*(\omega) = Z'(\omega) + iZ''(\omega)$) was converted into complex conductivity ($\sigma^*(\omega) = \sigma'(\omega) + i\sigma''(\omega)$) and complex permittivity ($\varepsilon^*(\omega) = \varepsilon'(\omega) - i\varepsilon''(\omega)$) using the equations $\sigma^*(\omega) = k[Z^*(\omega)]^{-1}$ and $\sigma^*(\omega) = i\omega\varepsilon_o\varepsilon^*\omega$, respectively, where k was the cell constant and $\omega = 2\pi f$ (f was the frequency in Hz).[8]

Broadband electric spectra were measured as a function of CO_2 pressure at 40°C from 0 to 60 bar as previously described[9] and summarized here. The measurements were made in a homemade high CO_2 pressure cell.[9] The gas was pre-dried over a type-A zeolite bed in order to exclude any traces of water from the CO_2, which could give rise to proton conductivity in the materials. This measurement setup allowed the measurements to be performed on extremely moisture sensitive materials such as PEO-based polymer electrolytes in totally anhydrous conditions[7]. A manual screw pump allowed the cell pressure to be increased to pressures higher than the gas cylinder. The pump was cooled by a thermostatic bath to maintain the CO_2 in a subcooled condition (ca. 278 K). The temperature of the high CO_2 pressure cell was controlled by a second thermostatic bath within ±0.05 °C and was monitored by a resistance sensor. The high CO_2 pressure (HCP) was monitored by a Bourdon gauge. The experimental electric spectra were recorded by an Agilent 4284A Precision Impedance Analyser in the frequency range from 20 Hz to 1 MHz.

QUANTUM MECHANICAL CALCULATIONS.

The vibrational spectra of the TOFA cation and the mono-substituted cation were determined via first-principle calculations using density functional theory methods implemented in an all-electron DFT code using the DMol3 program[10, 11] as a part of the Materials Studio package (double numerical plus polarization basis set, gradient-corrected (GGA) BLYP functional). The vibrational modes were identified by animating the atomic motions of each calculated mode using features available in the DMol3 package.

Results and discussion

Thermal Analysis.

The thermal properties of TOFATFSI were determined with TG and DSC. The TG profile, shown in Figure 1, exhibits five mass eliminations between 80 and 500°C. The overall thermal stability of this ionic liquid is quite low in comparison to other TFSI-containing ILs. TFSI-containing ILs tend to start thermal decomposition between 250 and 400°C[12-15]. In comparison, the TG profile of LiTFSI[16] does not exhibit a significant mass loss until 340°C. Therefore it would seem that the low thermal

View Article Online
DOI: 10.1039/C7CP02304A

decomposition of TOFATFSI is not due to the anion, but instead the stability of the cation and eventually to traces of other side products. The synthesis procedure used here is direct transamination, which is a slow process. Thus clearly some of the starting materials are still present, i.e. dioctylamine, and also the mono-substituted cation $[(C_8H_{17})_2NCHNH_2]^+$ resulting

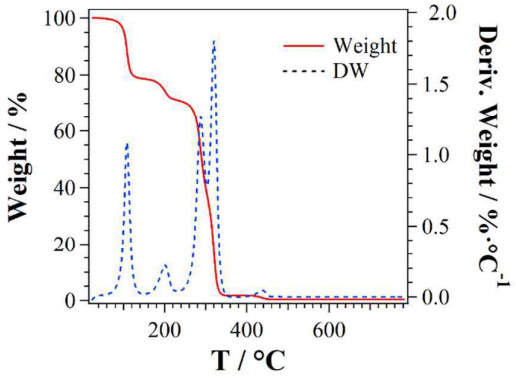

Figure 1. TG profile of TOFATFSI. Wt% is shown on the left axis and the derivative of wt% is shown on the right axis.

from partial substitution as confirmed by the existence of a weak peak at frequencies attributed to C-NH_2 (see the IR section below). However, the presence of these impurities is not likely to contribute to either the miscibility or the generation of ions.

If interest in this material for practical application arises, new synthetic procedures should be devised to obtain an IL with very high purity. However, the magnitude of mass loss, which occurs at ca. 100°C and is approximately 20 wt%, is much too large to be attributed to the traces of solvents and above described impurity losses. As a result, the first elimination likely marks the beginning of the cation decomposition. A similar TFSI-based ionic liquid, which contained a trioctyl(perfluorooctyl)ammonium cation, had a much higher thermal stability (358°C) than TOFATFSI.[14] This result may indicate that the low thermal decomposition maybe related to N-CH-N center of the cation which contains the delocalized positive charge, or to the presence of impurities. A thorough ^{1}H and ^{13}C NMR along with ^{1}H-^{13}C heteronuclear multiple-quantum correlation (HMQC) 2D analysis (see supplementary information) of an aged sample of TOFATFSI showed that there are substantial amounts of unreacted amines and monosubstituted amidinium salt. This could be due to unreacted amine or de-alkylation because the sample tested is aged. However these impurities are not ionized and do not contribute to the conductivity in alkane nor in super-critical CO_2. Similar issues with purity was also observed by some of the authors in a recent work on other members of the amidinium imide family.[17]

The DSC profile of TOFATFSI is shown in Figure 2. There is only one thermal event, a glass transition at ca. -75°C, in the investigated temperature range. It is important to note that there is no evidence of any endothermic peaks in the DSC curve, which indicates that TOFATFSI exists as a liquid in this temperature range.

It is well known that many ILs can exist in a supercooled state well below their melting point. In this case, the crystallization is likely severely hindered by both the conformational flexibility of the octyl groups in the bulky TOFA cation.[18, 19] Similar behaviour is also seen in the trioctyl(perfluorooctyl)ammonium TFSI ionic liquid described above.[14]

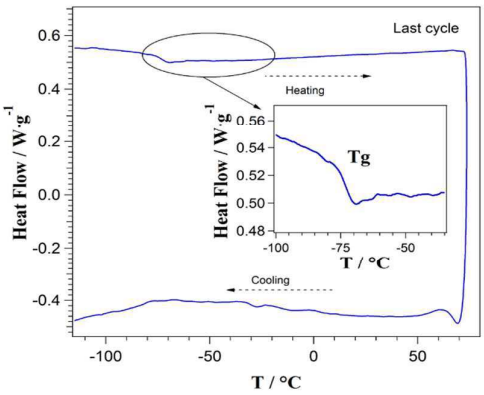

Figure 2. DSC profile of TOFATFSI. The inset shows an expanded view of the glass transition, T_g.

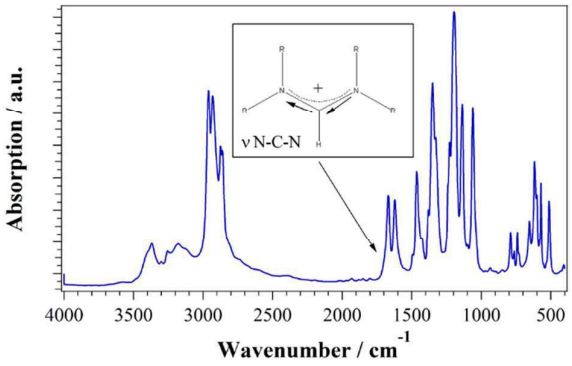

Figure 3. IR profile of TOFATFSI. The inset illustrates one of the cation N-C-N stretching modes.

Vibrational Spectroscopy

The infrared spectrum of TOFATFSI is shown in Figure 3 and the band assignments can be found in Table 1.

The vibrational spectrum of the TFSI anion has already been extensively studied[20-25] and these vibrational assignments[20] have been used to identify the anion modes visible in the spectrum of TOFATFSI. The frequencies of the anion modes are largely unchanged, within the error of the instrument, from those identified in other TFSI-containing systems, such as PEO electrolytes.[20] However, this result is not particularly surprising as the vibrational modes of anions with lower symmetry, such as TFSI, are not as sensitive to interactions within the system as those anions with higher symmetry,[26] such as PF_6^- or $CF_3SO_3^-$.

View Article Online
DOI: 10.1039/C7CP02304A

Several other peaks are visible within the spectrum of Figure 3 which can be associated with the TOFA cation. Several bands typical of alkanes, such as the stretching and bending modes of the methyl and methylene units of the octyl substituent chains are found in the frequency ranges of 2800 – 3000 cm^{-1} and 1380 – 1500 cm^{-1}, respectively.

The frequency ranges of these moieties are well within those typically reported.[27] In addition, the extended methylene rocking mode associated with the octyl groups can be identified at 729 cm^{-1}. Aside from these few peaks, it is difficult to associate any other bands of the TOFATFSI IR spectrum with the alkyl moieties likely due to the low intensity expected of the low frequency (below 1300 cm^{-1}) alkane modes in the infrared spectrum.[27]

Several bands can be associated with the N-CH-N centre of the cation which contains the delocalized positive charge. There are two peaks at 1622 and 1670 cm^{-1}, which are assigned to symmetric and asymmetric N-C-N stretching modes, respectively. The frequency of these modes is consistent with those typically seen in imine-type compounds[27] and reflects a bond order that is in between single and double as would be expected of these CN bonds due to the delocalization of the positive charge over all three atoms. The other mode assignments associated with the central part of the cation were made based on quantum chemical calculations using the DMol3 package[10, 11] within the Materials Studio Suite. In comparison with the low frequency alkyl modes, the lower frequency modes of this part of the cation are of a slightly higher intensity, likely due to a larger dipole moment derivative, as would be expected.

Table 1. Vibrational Assignments of the experimental TOFATFSI FT-IR spectrum.

Assignment*			
Experimental	Cation	Anion	Ref
408 (vw)		ωSO_2	[20]
512 (w)		$\delta_{as}CF_3$	[20]
570 (w)		$\delta_{as}CF_3$	[20]
600 (w)		$\delta_{as}{}^{ip}SO_2$	[20]
617 (m)		$\delta_{as}{}^{op}SO_2$	[20]
654 (w)		δSNS	[20]
729 (vw)	ρCH_2		[27]
740 (w)		TFSI E-C mode$	[23]
763 (vw)		ν_sSNS	[20]
789 (w)		νCS	[20]
849 (vw)	νN-C(R)		†
935 (vw)	$\delta^{op}CH$		†
1060 (s)		ν_{as}SNS	[20]
1135 (s)		$\nu_s SO_2$	[20]
1195 (vs)		$\nu_{as}CF_3$	[20]
1226 (m)		$\nu_{as}CF_3$	[20]
1328 (m)		$\nu_{as}{}^{ip}SO_2$	[20]
1350 (s)		$\nu_{as}{}^{op}SO_2$	[20]
1381 (w)	$\delta_s CH_3 + \omega CH_2$		[27]†
1427 (vw)	$\delta^{ip}CH$		†
1465 (m)	$\delta_{as}CH_3 + \delta CH_2$		[27]
§1593 (sh)	δNH_2		‡
1622 (w)	ν_sNCN		[27]†
1671 (w)	ν_{as}NCN		[27]†
§1696 (sh)	νNCN		‡
2861 (m)	$\nu_s CH_2$		[27]
2875 (m)	$\nu_s CH_3$		[27]
2935 (s)	$\nu_{as}CH_2$		[27]
2962 (s)	$\nu_{as}CH_3$		[27]
§3124 (vw), §3180 (vw), §3255 (vw)	νNH_2 interacting with the TFSI anion		
§3369 (vw)	$\nu_s NH_2$		[27]‡
§3405 (sh)	$\nu_{as}NH_2$		[27]‡

*The following symbols represent: ν – stretching mode, δ – bending mode, ω – wagging mode, ρ – rocking mode, s – symmetric, as – asymmetric, ip – in-plane, op – out-of-plane, § – mode belonging to mono-substituted cation.

#The following symbols represent: vs – very strong, s – shoulder, m – medium, w – weak, vw – very weak, sh – shoulder.

$TFSI-expansion-contraction mode[25]

† Correlative assignments made based on a DMol3 quantum chemical calculation of IL cation.

‡ Correlative assignments made based on a DMol3 quantum chemical calculation of mono-substituted cation.

As a result, it is easier to differentiate these cation peaks, in particular the C-H in-plane and out-of-plane bending modes, from the rest of the spectrum.

There are some peaks above 3000 cm^{-1} that are more difficult to assign. This region of the TOFATFSI spectrum should not contain any peaks based on the structure of the ionic liquid. The presence of bands in this region suggests that there is small amount of TOFA cations that are mono-substituted due to an incomplete reaction of the amidine precursor with dioctyl amine during the synthesis process. This would leave

View Article Online
DOI: 10.1039/C7CP02304A

NH_2 moieties on some of the cations. Therefore, the bands at 3405 and 3369 cm^{-1} correspond to the asymmetric and symmetric stretching motion of NH_2 groups that are very weakly interacting with the anion. These frequencies are in good agreement with those typically accepted for primary amines in dilute solutions.[27] The peaks between 3300 and 3000 cm^{-1} are likely associated with NH_2 groups that are more strongly interacting with the TFSI anion. The peaks in the lower end of this frequency region could be enhanced by Fermi resonance with the first overtone of the NH_2 deformation.[27] The presence of the mono-substituted TOFA cations is also evident in the spectral region containing the N-CH-N stretching modes. The deconvolution of this spectral region is shown in Figure 4.

There are shoulders on both sides of the N-CH-N stretching peaks previously assigned to the TOFA cation. The high frequency shoulder at 1696 cm^{-1} corresponds to the N-CH-NH_2 stretching mode, while the low frequency shoulder at 1593 cm^{-1} corresponds to the NH_2 deformation. These frequencies are consistent with the frequencies calculated using the DMol3 program for the mono-substituted cation. Given the intensity of the peaks corresponding to the N-CH-NH_2 stretching mode in comparison to those of the TOFA N-CH-N stretching mode, it is reasonable that there is only a small percentage of the mono-substituted cation in the TOFATFSI sample.

Broadband Electrical Spectroscopy

BES as a Function of Temperature under Inert Atmosphere. The imaginary component of the permittivity (ε") and the real component of the conductivity (σ') as function of frequency at temperatures between -150 and 80°C are shown in parts (a) and (b) of Figures 5 for the TOFATFSI ionic liquid.

As the temperature increases, a peak with values of ε" ranging from 10^5 to 10^6 appears and moves toward higher frequencies. At temperatures below 40°C and frequencies above 100 Hz, the presence of dielectric relaxations is identified by an inflection point in ε".

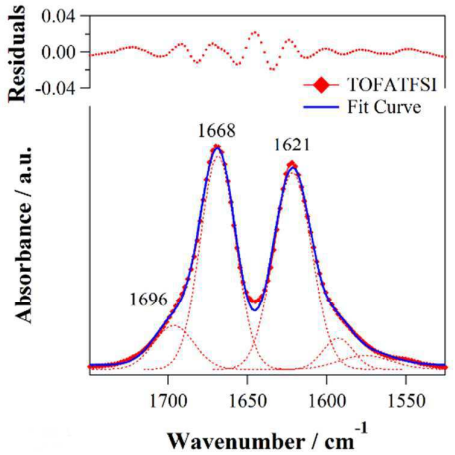

Figure 4. Deconvolution of N-CH-N stretching peaks of TOFATFSI FT-IR spectrum.

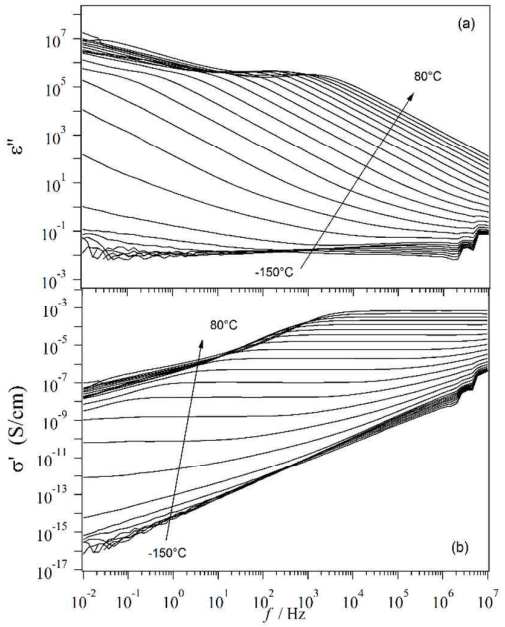

Figure 5. Profiles of ε" (part a) and σ' (part b) as a function of frequency at ambient pressure and temperatures between -150 and 80°C.

The profiles of σ', reported in Figure 5 part (b), show an inflection point that marks the beginning of a plateau that is correlated to the intense peaks in the ε" spectra. This plateau indicates the "bulk" conductivity, σ_{EP} ($\sigma_{EP} \approx \sigma_{DC}$), of the ionic liquid.[28] TOFATFSI has a conductivity of 6.7×10^{-5} and 6.6×10^{-4} $S\cdot cm^{-1}$ at 30 and 80°C, respectively. The presence of the intense peak in ε" and the corresponding decline in σ' indicates the presence of an electrode polarization event (EP). The EP is caused by the accumulation of charge at the interface between the blocking electrodes and electrolyte.[29] Profiles of σ' similar to those reported in Figure 5b were obtained for proton conducting ionic liquids and resulted from the combination of the bulk conductivity and the electrode polarization phenomenon.[30]

It is reasonable to hypothesize that the long-range conduction in TOFATFSI is modulated mainly by the motion of the anions based on: (1) the difference between the molecular weight and size of the IL cation and anion; and (2) the C_8H_{17} alkyl chains of the TOFA cation that tend to aggregate via Van der Waals interactions to form cation aggregates. The presence of cationic aggregates within the IL is proposed on the basis of the detected polarization event in ε*(ω) profiles with permittivity values higher than 10^6. This experimental evidence, as elsewhere demonstrated[31, 32], supports the hypothesis of the presence of cation and anion fluctuating nanoaggregates in bulk IL.

The dielectric relaxations are detected by analysing the profiles of the real part of permittivity ε', reported in Figure 6a. The ε' spectra reveal two dielectric relaxations, labelled α and β, which are identified by a step-decrease of the permittivity with increasing frequency. The β relaxation appears at lower temperatures than the α relaxation (Figure 6b). The intense feature shown in low frequency wing of the spectra (Figure 5a)

View Article Online
DOI: 10.1039/C7CP02304A

that exhibits a step-like decrease in ε' with values dropping from 10^6 to 10 is associated with the EP phenomenon.

The presence of the α and β relaxations is confirmed by the examination of the tanδ = ε''/ε' profiles plotted as a function of temperature at 10Hz, 100Hz and 10 kHz as reported in Figure 7.

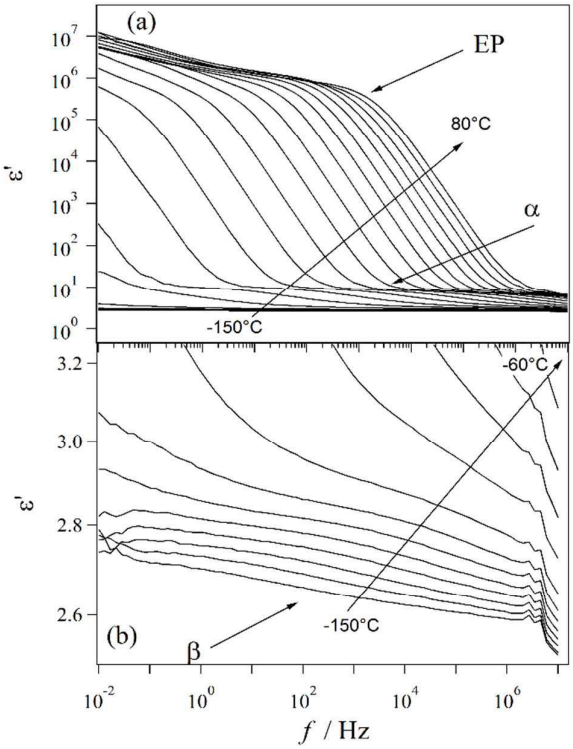

Figure 6. Profiles of ε' as a function of frequency at ambient pressure and at temperatures between: (a) -150 and 80°C; (b) -150 and -60°C.

Two peaks are evident in the tanδ profiles: the β relaxation (-150 – -80°C) and the α relaxation (-80 – 50°C). The α relaxation appears at temperatures above the glass transition temperature T_g (-75°C) of the material and may be associated with an order-disorder transition due to a long-range diffusion of conformational states of the octyl groups or diffusion of structural defects between cation aggregates of TOFATFSI. The β relaxation appears at lower temperatures and is the result of faster dynamics than the α transition. The β relaxation is associated with local rotational fluctuations of the octyl groups related to the "bulk" relaxation modes of the single TOFA cations.

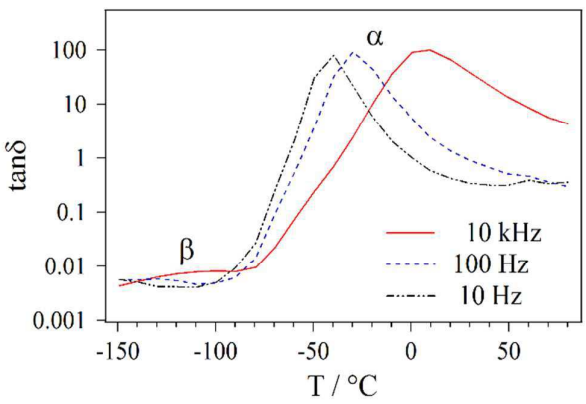

Figure 7. Profiles of tanδ as a function of temperature at 10Hz, 100Hz and 10 kHz.

The conductivity values associated with the EP polarization event, the dielectric strengths and the characteristic relaxations times are obtained by fitting the experimental profiles of $\varepsilon(\omega) = \varepsilon'(\omega) - i\varepsilon''(\omega)$ with Equation 1.[28]

$$\varepsilon^*(\omega) = \frac{\sigma_{EP}(i\omega\tau_{EP})^{\gamma}}{i\omega[1+(i\omega\tau_{EP})^{\gamma}]} + \sum_{j=1}^{2}\frac{\Delta\varepsilon_j}{\left[1+(i\omega\tau_j)^{\mu_j}\right]} + \varepsilon_\infty \qquad (1)$$

The first term describes the electrode polarization phenomenon. The variables σ_{EP} and τ_{EP} are the conductivity and relaxation time associated with the EP event, while γ is a shape parameter that describes the broadness and asymmetry of the EP peak. The second term expresses the dielectric relaxations through a Cole-Cole type equation,[33] where j corresponds to α or β-modes. ω= 2π*f* is the angular frequency of the electric field, τ_j is the relation time of the j^{th} event of intensity $\Delta\varepsilon_j$, and μ_j is a shape parameter bound to the distribution of the relaxation times associated with the j^{th} event. The third term, ε_∞, is the electronic contribution to the permittivity of the material. Equation 1 is used to simultaneously fit the experimental tanδ, ε', ε", σ' and σ" spectra which are determined from the permittivity spectra according to the relationship between the complex conductivity and complex permittivity: $\sigma^* = i\omega\varepsilon_0\varepsilon^*$.

The logarithmic values of σ_{EP} and f_{EP}=1/(2πτ_{EP}) are reported as a function of the reciprocal temperature in Figure 8. The σ_{EP} values correspond to those read directly from the high frequency plateau of the σ' spectra. The values of logσ_{EP} and logf_{EP} as a function of T^{-1} have a Vogel–Tammann–Fulcher (VTF) dependence.[8]

The pseudo-activation energy and the temperature T_0 obtained from the fit parameters are 15.0±0.3 kJ/mol and 141±1 K for σ_{EP} and 15±1 kJ/mol and 139±3 K for f_{EP}. As typically reported in literature for polymer electrolytes,[8] the value of T_o (-133°C) is about 60°C lower than the glass transition temperature.

The dielectric strengths and the relaxation times associated with the α and β transitions at different temperatures can be determined from the second term of Equation 1. Logf_j and $\Delta\varepsilon_j$

View Article Online
DOI: 10.1039/C7CP02304A

as a function of reciprocal temperature, where j corresponds to α or β, are shown in Figure 9 a and b.

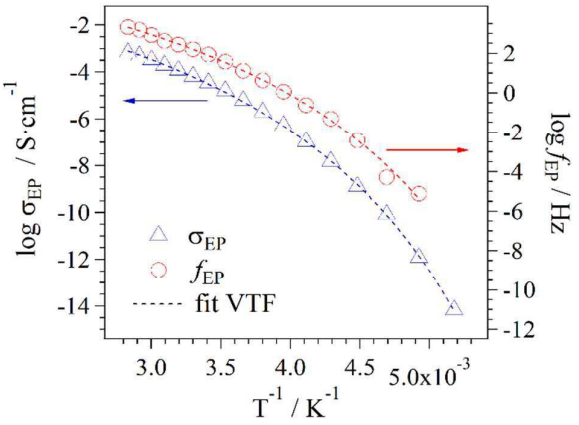

Figure 8 Logarithmic values of σ_{DC} and f_{EP} =1/(2π τ_{EP}) as a function of reciprocal temperature.

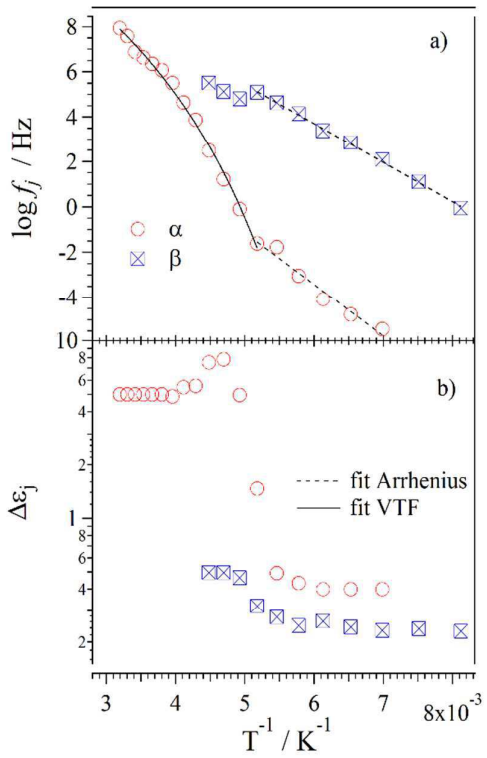

Figure 9. Values of logf_j (a) and $\Delta\varepsilon_j$ (b) as a function of reciprocal temperature.

$\Delta\varepsilon_\beta$ increases slightly with temperature and is lower than $\Delta\varepsilon_\alpha$. Above the Tg, $\Delta\varepsilon_\alpha$ increases by one order of magnitude. Logf_β as function of T^{-1} follows Arrhenius behaviour with an activation energy of 33±1 kJ/mol. Logf_α vs. T^{-1} shows Arrhenius behaviour below the glass transition temperature, but changes to VTF behaviour above T_g. The activation energy $E_{\alpha,Arr}$ = 44±4 kJ/mol and pseudo-activation energy $E_{\alpha,VTF}$ = 23±3 kJ/mol are obtained from fitting the data with the Arrhenius (at $T < T_g$) and VTF (at $T > T_g$) equations,[8] respectively. $E_{\alpha,VTF}$ is reasonably close to the pseudo-activation energy of the ionic conduction (15 kJ/mol, Figure 8). This result indicates that the α relaxation corresponds to the diffusion of structural defects between ion aggregates. The α mode is coupled with the long-range charge migration events, which are largely related to the anion migration phenomena. Finally, the values of ε_∞ (data not shown), derived from fitting the data with equation 1, vary slightly with temperature from 2.5 at -150°C to 3.4 at 80°C. The correlation existing between the α mode and the long-range charge transfer processes supports the hypothesis that interacting alkyl chains, forming cationic aggregates, are playing a crucial role in the modulation of the overall conductivity mechanism of the IL. Nevertheless, the shape and the size of these cationic aggregates should be confirmed and studied by other structural or spectroscopic investigations.

Effect of the CO_2 Pressure at Constant Temperature on the Electric Properties of TOFATFSI.

The profiles of ε', ε'' and σ', collected at 40°C as function of frequency at different CO_2 pressures (between 0 and 60 bar), are reported in Figure 10 a, b and c, respectively.

The spectra in Figure 10 show the presence of the electrode polarization phenomenon as indicated by: a) a peak in ε" with values ranging from 10^5 to 10^6; b) an inflection point that marks

View Article Online
DOI: 10.1039/C7CP02304A

Journal Name

ARTICLE

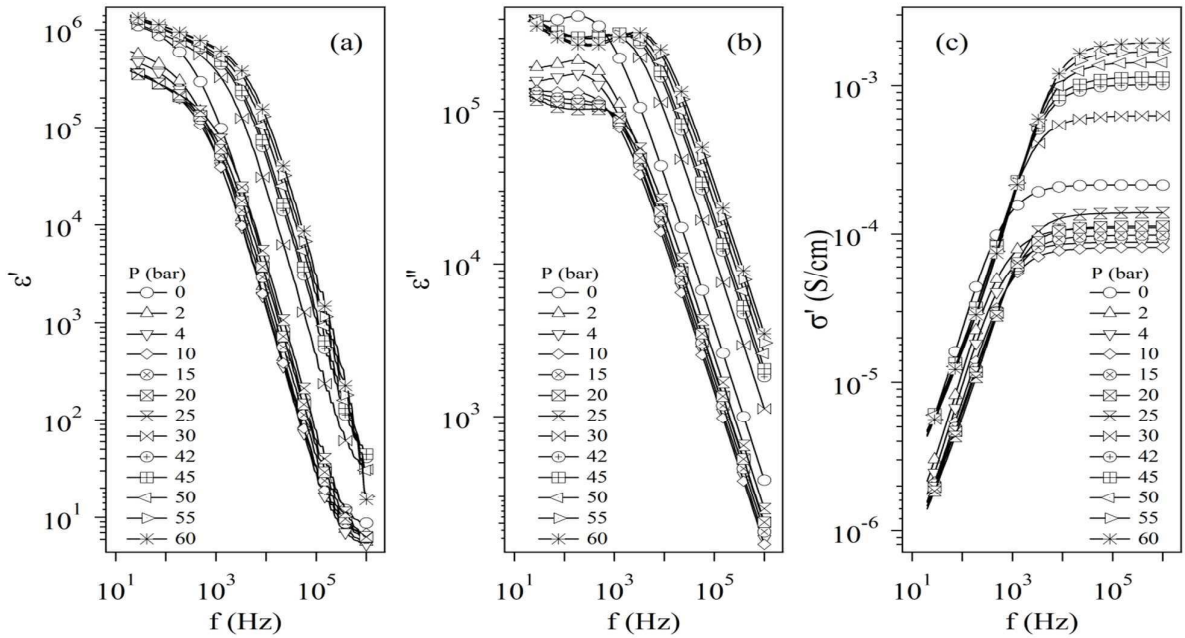

Figure 10. Profiles of ε' (a), ε'' (b) and σ' (c) as a function of frequency at pressures between 0 and 60 bar CO_2.

the beginning of a plateau in σ'; and c) a step-like decrease of ε' with values dropping from 10^6 to 10. Recall from Section 3.3.1 that EP is associated with charge accumulation at the ionic liquid-electrode interfaces and is related to the "bulk" conductivity, $\sigma_{EP,}$ of the material. The values of σ_{EP} and the relaxation times, $\tau_{EP,}$ associated with the electrode polarization are obtained by fitting the experimental data with the first term of Equation 1. Logσ_{EP} and logf_{EP} are reported as function of the CO_2 pressure in Figure 11a and b, respectively. The trend of logσ_{EP} can be divided into three distinct regions, labelled I, II and III. In region I between 0 and 10 Bar, the conductivity and the frequency f_{EP} decrease with increasing CO_2 pressure. This effect is due to the diffusion of CO_2 into bulk material, which reduces the local permittivity and allows interactions between the alkyl chains within the cation aggregates. A higher degree of interactions in a low permittivity environment is expected to reduce the alkyl chain flexibility thus influencing the relaxation phenomena responsible for the long range anion migration events.[34]

In region II from 10 to 25 bar, the conductivity of the ionic liquid increases linearly with the gas pressure from 7.9×10^{-5} S·cm^{-1} at 10 bar to 1.5×10^{-4} S·cm^{-1} at 25 bar. In this region a critical concentration of CO_2 in the bulk of TOFATFSI is reached, which progressively modifies the structure of the ionic aggregates. The further plasticizing effect of the CO_2 results in a gradual increase in the size of the ionic aggregates which improves the delocalization of anions through a solvation effect and increases the density and mobility of the charge carriers "free to move". This is in accordance with other studies and suggests that the "delocalization body" increases in size with increasing P_{CO2} in this region.[35] The delocalization body consists of the volume including the cation aggregates and interstitial anion domains, where the anion can be considered to be delocalized in the time scale of conductivity.

There is a step-like increase in the conductivity between region II and region III from 1.5×10^{-4} to 6.7×10^{-4} S·cm^{-1}. In region III above P_{CO2} = 30 bar, the conductivity increases linearly with the gas pressure. This step increase corresponds to incorporation of an excess of liquid CO_2 into the lipophilic domains of cation aggregates. The excess liquid CO_2, which interacts with lipophilic moieties of the ionic liquid, increases the size of the cationic aggregates and the result is an increase of the volume of the delocalization body and thus a steep increase of the degree of delocalization of "free to move" charge carrier concentration (the anion). It is observed that the slope in region III is the same as the slope in region II, which indicates that the mechanism of the size increase of lipophilic aggregates in these two regions is similar.

The frequency, $f_{EP,}$ associated with the EP has the form:[36]

View Article Online
DOI: 10.1039/C7CP02304A

$$f_{EP} = \frac{\sigma_{EP}}{\varepsilon_0 \varepsilon_{EP}} \left(\frac{d_{EP}}{L}\right) \quad (2)$$

where σ_{EP} is the bulk conductivity, L is the sample length, ε_0 is the vacuum permittivity and ε_{EP} and d_{EP} are the complex permittivity and the thickness of the interfacial region, respectively. Typically, it is expected that d_{EP} is on the order of 1 nm for ionic liquids.[37] Equation 2 indicates that f_{EP} increases with increasing charge carrier concentration and mobility and decreases with the sample thickness L.[36] Figure 8 shows that the temperature dependence of f_{EP} exactly follows the temperature dependence of σ_{EP}. This suggests that temperature has the most significant effect on the conductivity as compared to all of the other parameters on the right side of Equation 2 and in particular increases the mobility as opposed to the concentration of the charge carriers. In contrast, f_{EP} as a function of pressure does not follow the same behaviour as the conductivity as it does not exhibit the same step-like increase as the conductivity between region II to region III (Figure 11).

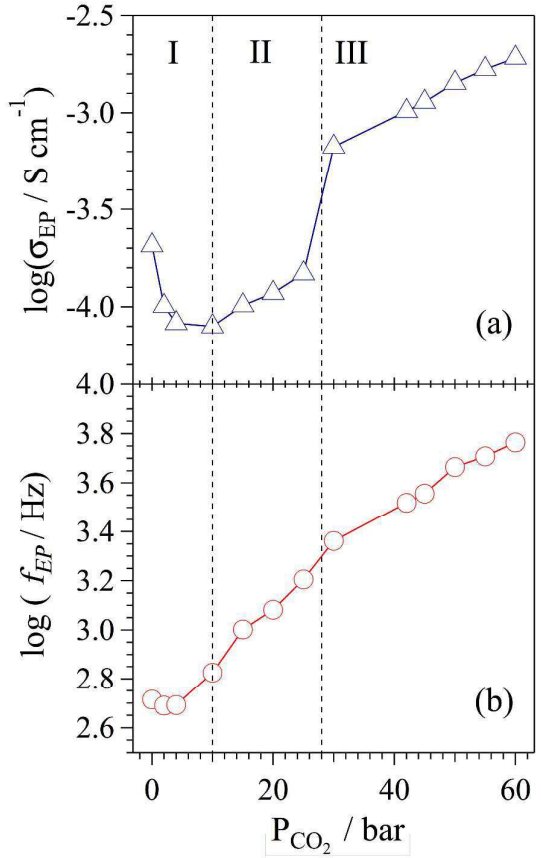

Figure 11. Logarithmic values of σ_{EP} (a) and $f_{EP} = 1/2\pi\tau_{EP}$ (b) as a function of the CO_2 pressure at 40°C.

In considering Equation 2, this is possible if it is reasonable to assume that the increase of ε_{EP} in region III arises from an increase in the density of charge carriers accumulating at the electrode-electrolyte interface associated with a progressive increase of the size of the ionic nanoaggregates.

From Equation 2, it is possible to calculate ε_{EP} using the values of σ_{EP} and f_{EP}, determined by fitting the experimental data with Equation 1, and by assuming that d_{EP} = 1 nm [23] and L = 200μm. The values of ε_{EP} as function of temperature and pressure are calculated using the values of σ_{EP} and f_{EP} reported in Figures 8 and 11, respectively. Figure 12a and b show the trend of ε_{EP} as a function of temperature and pressure, respectively.

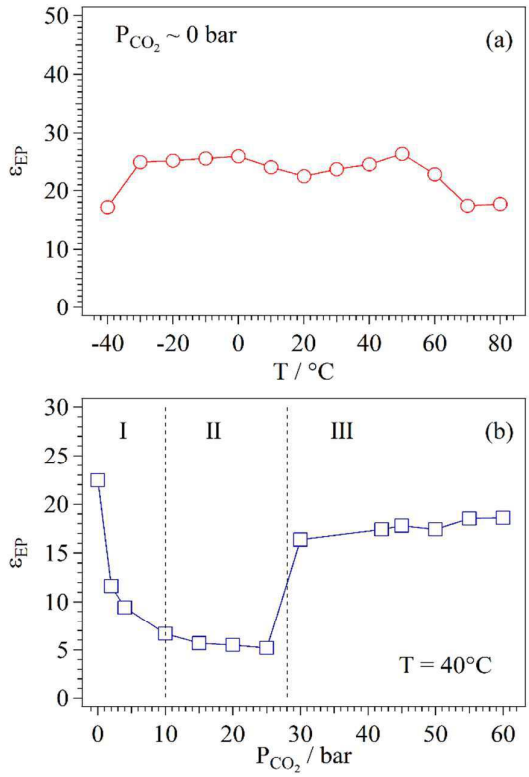

Figure 12. Values of ε_{EP} as a function of the temperature (a) and the CO_2 pressure (b).

ε_{EP} slightly changes as a function of temperature and has values of ca. 25. At $P_{CO2} \approx 0$ bar, the temperature does not affect the concentration of charge carriers accumulated at the electrode. In contrast, at T=40°C, ε_{EP} exhibits a dependence on P_{CO2} (Figure 12b). In region I (0 – 10 bar), ε_{EP} decreases with increasing CO_2 pressure due to the diffusion of CO_2 into the lipophilic cation aggregates of the bulk TOFATFSI which causes the size of cation aggregates to shrink due to the attractive dispersive interactions and reduces the amount of charge accumulating at the TOFATFSI-electrode interface. In region II (between 10 and 25 bar) ε_{EP} slightly decreases with CO_2 pressure, which indicates an increase of the TOFATFSI lipophilic character associated with the presence of interstitial CO_2 inside the cation aggregates which are slightly increasing in size. In region III (above 30 bar), ε_{EP} increases with increasing CO_2 pressure, which suggests that above 25 bar the liquid CO_2 domains act as a solvent seed for the reorganization of the alkyl groups of cationic aggregates.

Thus, the size of the delocalization bodies increases and improves the anion charge delocalization phenomena, which

View Article Online
DOI: 10.1039/C7CP02304A

in turn facilitates the charge density accumulating at the electrode interface.

Conclusions

The work describes the preparation a new lipophilic ionic liquid which is miscible with hydrocarbons and exhibits an acceptable ionic conductivity for practical application in various electrochemical devices. Of particular interest is the investigation of the behaviour of the IL in the challenging highly apolar environment. The TOFA cation is characterized by a positive charge delocalized over the N-CH-N portion of the cation as indicated by a N-CH-N stretching frequency that is similar to those in imine-like compounds, which reflects the bond order of the C-N bonds that is somewhere between single and double bond order. In addition, the FT-IR spectrum reveals that there is small percentage of a mono-substituted cation present within the TOFATFSI material. This cation has been identified by peaks in both the NH_2 and N-CH-N stretching regions. It should be reiterated that although a more pure material would be needed for a practical electrochemical application, the presence of this small amount of side products does not affect the investigation of the structural organization of the ions within IL.

The conductivity and relaxation phenomena are realized through the BES analysis, which reveals a bulk conductivity and two dielectric relaxations: α and β. The α relaxation appears above the glass transition and may be associated with an order-disorder transition due to long-range conformational diffusion of the alkyl groups or diffusion of structural defects in the cationic aggregates. The β relaxation that appears at lower temperatures is associated with rotational fluctuations of the octyl groups related to the local "bulk" relaxation modes of the TOFA cations. BES spectroscopy is a very powerful technique that is used here to elucidate the effect of temperature and CO_2 uptake on the IL conductivity. Temperature increases the conductivity via an increase in the charge carrier mobility. CO_2 absorption affects both the conductivity and the permittivity of the material due to the presence of CO_2-IL interactions that modulate the nanostructure and the size of the TOFATFSI aggregates, which increases both the mobility and the density of the charge carriers. Finally, the long range charge migration in TOFATFSI occurs via the exchange of interstitial delocalized anions between delocalization bodies. These delocalization bodies consist of cation aggregates with the anions immersed in the interstitial domains. On the basis of the similarity of the values of the activation energy of the α-mode and pseudo-activation energy of σ, the exchange of anions between delocalization bodies is significantly modulated by α-relaxation (segmental motion) of IL.

Acknowledgements

This work was supported by Strategic Project of the University of Padova "Materials for Membrane-Electrode Assemblies to Electric Energy Conversion and Storage Devices (MAESTRA)".

The authors like to thank Dr. Ileana Menegazzo for the NMR measurements and Mr. Gilles Robertson for his help in the analysis of NMR results.

References

1. D. R. MacFarlane, N. Tachikawa, M. Forsyth, J. M. Pringle, P. C. Howlett, G. D. Elliott, J. H. Davis, M. Watanabe, P. Simon and C. A. Angell, *Energy & Environmental Science*, 2014, **7**, 232-250.
2. A. Ponrouch, D. Monti, A. Boschin, B. Steen, P. Johansson and M. R. Palacin, *Journal of Materials Chemistry A*, 2015, **3**, 22-42.
3. G. A. Giffin, *Journal of Materials Chemistry A*, 2016, **4**, 13378-13389.
4. M. A. Steffen Hess, Margret Wohlfahrt-Mehrens, Gerhard Maas, and Mario Wachtler, *Journal of Electrochemical Society*, 2014, **161**, 9.
5. D. P. Milen G. Bogdanov, Stanimira Hristeva, Ivan Svinyarov, Willi Kantlehner, *Zeitschrift für Naturforschung B*, 2010, **65b**, 12.
6. N. M. M. Mateus, L. C. Branco, N. M. T. Lourenco and C. A. M. Afonso, *Green Chemistry*, 2003, **5**, 347-352.
7. S. Kitajima, F. Bertasi, K. Vezzu, E. Negro, Y. Tominaga and V. Di Noto, *Physical Chemistry Chemical Physics*, 2013, **15**, 16626-16633.
8. V. Di Noto, *Journal of Physical Chemistry B*, 2002, **106**, 11139-11154.
9. V. Di Noto, K. Vezzù, F. Conti, G. A. Giffin, S. Lavina and A. Bertucco, *The Journal of Physical Chemistry B*, 2011, **115**, 9014-9021.
10. B. Delley, *The Journal of Chemical Physics*, 1990, **92**, 508-517.
11. B. Delley, *The Journal of Chemical Physics*, 2000, **113**, 7756-7764.
12. M. A. B. H. Susan, A. Noda and M. Watanabe, in *Electrochemical Aspects of Ionic Liquids*, John Wiley & Sons, Inc., 2005, DOI: 10.1002/0471762512.ch5, pp. 55-74.
13. M. B. Herath, T. Hickman, S. E. Creager and D. D. DesMarteau, *Journal of Fluorine Chemistry*, 2011, **132**, 52-56.
14. H. Xue, R. Verma and J. n. M. Shreeve, *Journal of Fluorine Chemistry*, 2006, **127**, 159-176.
15. K. Liu, Y.-X. Zhou, H.-B. Han, S.-S. Zhou, W.-F. Feng, J. Nie, H. Li, X.-J. Huang, M. Armand and Z.-B. Zhou, *Electrochimica Acta*, 2010, **55**, 7145-7151.
16. Z. Lu, L. Yang and Y. Guo, *Journal of Power Sources*, 2006, **156**, 555-559.
17. Y. Abu-Lebdeh, A. Hammami, A. Abouimrane and M. Armand, *Electrochemistry Communications*, 2017, **81**, 112-115.
18. W. A. Henderson and S. Passerini, *Chemistry of Materials*, 2004, **16**, 2881-2885.
19. A. Triolo, O. Russina, B. Fazio, G. B. Appetecchi, M. Carewska and S. Passerini, *Journal of Chemical Physics*, 2009, **130**, 164521.
20. I. Rey, P. Johansson, J. Lindgren, J. C. Lassègues, J. Grondin and L. Servant, *The Journal of Physical Chemistry A*, 1998, **102**, 3249-3258.

View Article Online
DOI: 10.1039/C7CP02304A

21. K. Fujii, T. Fujimori, T. Takamuku, R. Kanzaki, Y. Umebayashi and S.-i. Ishiguro, *The Journal of Physical Chemistry B*, 2006, **110**, 8179-8183.
22. M. Herstedt, M. Smirnov, P. Johansson, M. Chami, J. Grondin, L. Servant and J. C. Lassègues, *Journal of Raman Spectroscopy*, 2005, **36**, 762-770.
23. J. C. Lassègues, J. Grondin, R. Holomb and P. Johansson, *Journal of Raman Spectroscopy*, 2007, **38**, 551-558.
24. P. Johansson, J. Tegenfeldt and J. Lindgren, *The Journal of Physical Chemistry A*, 2000, **104**, 954-961.
25. D. Brouillette, D. E. Irish, N. J. Taylor, G. Perron, M. Odziemkowski and J. E. Desnoyers, *Physical Chemistry Chemical Physics*, 2002, **4**, 6063-6071.
26. J. Grondin, J.-C. Lassègues, D. Cavagnat, T. Buffeteau, P. Johansson and R. Holomb, *Journal of Raman Spectroscopy*, 2011, **42**, 733-743.
27. D. Lin-Vien, N. B. Colthup, W. G. Fateley and J. G. Grasselli, *The Handbook of Infrared and Raman Characteristic Frequencies of Organic Molecules*, Academic Press, San Diego, 1991.
28. F. Bertasi, K. Vezzù, G. Nawn, G. Pagot and V. Di Noto, *Electrochimica Acta*, 2016, **219**, 152-162.
29. G. Pagot, F. Bertasi, K. Vezzù, F. Sepehr, X. Luo, G. Nawn, E. Negro, S. J. Paddison and V. D. Noto, *Electrochimica Acta*, 2017, **246**, 914-923.
30. V. Di Noto, M. Piga, G. A. Giffin, S. Lavina, E. S. Smotkin, J.-Y. Sanchez and C. Iojoiu, *The Journal of Physical Chemistry C*, 2012, **116**, 1370-1379.
31. M. Kunze, S. Jeong, E. Paillard, M. Schönhoff, M. Winter and S. Passerini, *Advanced Energy Materials*, 2011, **1**, 274-281.
32. M. Collinet-Fressancourt, L. Leclercq, P. Bauduin, J.-M. Aubry and V. Nardello-Rataj, *The Journal of Physical Chemistry B*, 2011, **115**, 11619-11630.
33. V. Di Noto, G. A. Giffin, K. Vezzù, M. Piga and S. Lavina, in *Solid State Proton Conductors*, John Wiley & Sons, Ltd, 2012, DOI: 10.1002/9781119962502.ch5, pp. 109-183.
34. K. Vezzù, V. Zago, M. Vittadello, A. Bertucco and V. D. Noto, *Electrochimica Acta*, 2006, **51**, 1592-1601.
35. V. Di Noto, M. Piga, G. A. Giffin, K. Vezzù and T. A. Zawodzinski, *Journal of the American Chemical Society*, 2012, **134**, 19099-19107.
36. V. Di Noto, M. Piga, G. A. Giffin and G. Pace, *Journal of Membrane Science*, 2012, **390–391**, 58-67.
37. A. Schönhals and F. Kremer, in *Broadband Dielectric Spectroscopy*, eds. F. Kremer and A. Schönhals, Springer Berlin Heidelberg, Berlin, Heidelberg, 2003, DOI: 10.1007/978-3-642-56120-7_1, pp. 1-33.

View Article Online
DOI: 10.1039/C7CP02304A

Table of Content

A lipophilic ionic liquid based on formamidinium cations and TFSI: The electric response and the effect of CO_2 on conductivity mechanism

Federico Bertasi, Guinevere A. Giffin, Keti Vezzù, Pace Giuseppe, Yaser Abu-Lebdeh, Michel Armand, Vito Di Noto[*]

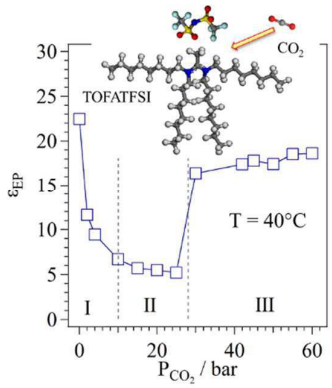

A new lipophilic ionic liquid tetraoctyl-formamidinium bis(trifluoromethanesulfonyl) imide (TOFATFSI) has been synthetizes and its interactions with a highly apolar environment of CO_2 are shown. CO_2 absorption affects both conductivity and permittivity due to the presence of CO_2-IL interactions that modulate the nanostructure and the size of the TOFATFSI aggregates, which increases both mobility and density of the charge carriers.